

Disappearance of Certain Acidic Organelles (Endosomes and Langerhans Cell Granules) Accompanies Loss of Antigen Processing Capacity upon Culture of Epidermal Langerhans Cells

By Hella Stössel, Franz Koch, Eckhart Kämpgen, Peter Stöger,
Angela Lenz, Christine Heufler, Nikolaus Romani,
and Gerold Schuler

From the Department of Dermatology, University of Innsbruck, A-6020 Innsbruck, Austria

Summary

Freshly isolated epidermal Langerhans cells (LC) can actively process native protein antigens, but are weak in sensitizing helper T cells. During culture, when LC mature into potent immunostimulatory dendritic cells, T cell sensitizing capacity develops but antigen processing capacity is downregulated. Processing of exogenous antigens for class II-restricted antigen presentation involves acidic organelles. We used the DAMP-technique to monitor acidic organelles at the ultrastructural level in fresh, as well as cultured, mouse and human LC. We observed that the loss of antigen processing capacity with culture of LC was reflected by the disappearance of certain acidic organelles, namely endosomes (particularly early ones), and the hitherto enigmatic LC granules ("Birbeck Granules"). Our findings support the notion that endosomes are critical for antigen processing and suggest that LC granules might be involved as well.

Dendritic cells (DC)¹ represent a distinct lineage of MHC class II-positive leukocytes specialized to initiate primary T cell responses (1, 2). DC occur in small numbers in most organs. It is currently believed that DC in nonlymphoid tissues (tissue DC) are the precursors of DC in lymphoid organs (lymphoid DC). Tissue DC are considered immature, as they do not exhibit the unique functional property of mature, lymphoid DC (i.e., the capacity to sensitize T cells). It is thought that they act as sentinels in the tissues by capturing and processing antigen (1, 2). After charging their surface MHC class II molecules with immunogenic peptides, they develop into potent immunostimulatory lymphoid DC, and home to the T areas of lymphoid organs to select and sensitize antigen-specific T cells from the circulating pool. The above concept is mainly derived from the observation that epidermal Langerhans cells (LC) develop into potent immunostimulatory DC upon 2–3 d of culture (3–5). Antigen presentation/processing and sensitizing function are reciprocally expressed in freshly isolated LC (fLC) vs. cultured LC (cLC) (6, 7). fLC (as in vitro equivalents of intraepidermal LC) can process native protein antigens, but are weak in stimulating resting T cells. Conversely, LC cultured for a total

of 48–72 h have lost the capacity to process antigen (at least in those mouse strains extensively studied so far) (6–8), but have acquired potent stimulatory capacity for resting T cells.

The precise localization of antigen processing (i.e., cleavage of exogenous antigens and binding to class II molecules) for class II-restricted presentation is not yet known (9, 10). Various experiments have indicated, however, that internalization into an acidic compartment is an essential step (11–13). We wondered whether the downregulation of antigen processing capacity during culture of LC was reflected by a change in the number or quality of acidic organelles. We used the so-called DAMP technique (14) to visualize acidic compartments at the ultrastructural level in fresh, as well as cultured, human and mouse LC. DAMP, i.e., 3-(2,4-dinitroanilino)-3'-amino-N-methyldipropylamine, is a specially formulated weak base that contains a DNP group. It readily diffuses into viable cells, is concentrated in acidic compartments, becomes covalently linked to proteins by aldehyde fixation, and can be detected by post-embedding immunolabeling using a suitable anti-dinitrophenyl mAb and protein A-gold. We found that two types of acidic organelles, namely endosomes (especially those of the early type) and LC granules (LCG) (Birbeck Granules), virtually disappeared upon culture of LC concomitant with the downregulation of antigen processing capacity. These organelles, therefore, may be the acidic intracellular compartments where critical steps in antigen processing by fLC occur.

¹ Abbreviations used in this paper: cLC, cultured LC; DAMP, 3-(2,4-dinitroanilino)-3'-amino-N-methyldipropylamine; DC, dendritic cell; fLC, freshly isolated LC; LC, epidermal Langerhans cells; LCG, LC granule; RT, room temperature.

Materials and Methods

Mice. BALB/c mice were purchased from Charles River Wiga (Sulzberg, FRG) and used at 6–10 wk of age.

Culture Medium. RPMI 1640 (Seromed-Biochrom, Berlin) was used, supplemented with 10% FCS (Gibco Laboratories, Paisley, Scotland), 50 μ M 2-ME (Sigma Chemical Co., St. Louis, MO), and 20 μ g/ml gentamicin (Gibco Laboratories).

Fresh Murine Langerhans Cells (fLC). Epidermal cell suspensions were prepared from ear skin by standard trypsinization (0.5% trypsin, 30–60 min, 37°C) (3). LC were enriched up to 15% by lysis of the majority of keratinocytes with anti-Thy-1 plus complement and subsequent removal of dead cells and debris by a brief trypsin (0.125%)/DNase (80 μ g/ml) treatment for 10 min at 37°C (15).

Cultured Murine Langerhans Cells (cLC). Bulk epidermal cells obtained by trypsinization were cultured for 3 d in 100-mm tissue culture dishes (3003; Falcon Labware, Oxnard, CA) in 10 ml of culture medium at a density of 2×10^7 cells per dish. Subsequently, LC were enriched up to 70% by flotation on dense BSA columns as described (3).

Viable Human Epidermal Sheets. Healthy human breast skin was obtained from corrective plastic surgery. Human split-thickness skin was floated on the bacterial enzyme Dispase (grade II; Boehringer Mannheim, Mannheim, FRG) at a final concentration of 1.2 U/ml in Eagle's MEM (Flow Laboratories, Inc., Irvine, Scotland). After 1 h at 37°C, the epidermis was peeled off with fine forceps. The resulting epidermal sheets were trimmed to a size of $\sim 2 \times 2$ mm and washed twice in PBS without calcium and magnesium.

Cultured Human Langerhans Cells (cLC). Human epidermal cell suspensions were prepared by standard trypsinization (overnight, 4°C, 0.25% trypsin) (16). Basal keratinocytes were removed by adherence (90 min/37°C) on collagen-coated tissue culture surfaces (Vitrogen 100; Collagen Corporation, Palo Alto, CA). The nonadherent cells were subjected to a brief shock treatment (vortex in ice-cold PBS) followed by 10 min/37°C of trypsin (0.125%)/DNase (80 μ g/ml) (17). This pre-enriched population, containing between 10% and 15% LC, was cultured at a density of 10^7 cells per 100 mm tissue culture dish (3003; Falcon Labware) in 10 ml of culture medium to which recombinant human granulocyte/macrophage CSF (GM-CSF) was added (400 U/ml; 10^7 U/mg sp act; a gift of Genetics Institute, Cambridge, MA). After 3 d, the nonadherent cells were collected, and cultured LC were further enriched to >80% by flotation on dense BSA columns (16).

Monitoring of Antigen Processing Capacity. Partially enriched fresh or cultured murine LC (see above) were pulsed for 12 h with 4 μ M sperm whale myoglobin (Fluka, Buchs, Switzerland) in the presence or absence of 100 μ M chloroquin or 25 μ M monensin (both from Sigma Chemical Co.) in culture medium. After three RPMI washes, graded doses of LC were plated in 96-well flat-bottomed microtest plates (Falcon Labware). 5×10^4 cells of the DBA/2-derived, I-E^d-restricted myoglobin peptide-specific T cell hybridoma 11.3.7 (18) (a gift of Dr. E. Puré, The Rockefeller University, New York, NY) were added to each well. Cells were cultured in 200 μ l culture medium with or without 3 μ M myoglobin peptide 110-121 (a gift of Dr. A. Livingstone, Basel Institute of Immunology, Basel, Switzerland). After 24 h, 100 μ l of culture supernatant was taken out from every well and IL-2 content assayed using the CTLL-2 cell line: 6×10^3 CTLL cells in 100 μ l of culture medium were added to 100 μ l of hybridoma culture supernatant in 96-well plates. After 32 h, cultures were pulsed with [³H]TdR (1 μ Ci/well, 6.7 Ci/mmol; New England Nuclear-DuPont Co., Boston, MA) for another 6 h. Data are means of triplicate wells in which SDs were <10%.

Postembedding Detection of Acidic Organelles. Viable epidermal sheets or viable single cell suspensions (enriched fractions of fLC or cLC) were first incubated with DAMP and subsequently fixed and processed for post-embedding immunogold labeling on ultrathin Epon sections. In extensive preliminary experiments, we had found that the use of Lowicryl sections, as described in the original publication (14), could be circumvented. By using optimal conditions, Epon sections even without etching gave an identical labeling density, but had the advantage of superior ultrastructure.

DAMP Treatment. A 6-mM stock solution of DAMP (Molecular Probes, Eugene, OR) was prepared in 100% ethanol. Both dispase sheets and cell suspensions were incubated in a 1:200 dilution of DAMP stock (i.e., 30 μ M final) in RPMI 1640 for 30 min at 37°C, followed by three washes in PBS. As controls, sheets and cells were incubated with DAMP in the presence of 100 μ M chloroquin or 25 μ M monensin (14). Then they were processed for electron microscopy.

Processing for Electron Microscopy. Both sheets and cell suspensions were: (a) fixed in Karnovsky's half-strength formaldehyde-glutaraldehyde fixative (1 h at room temperature [RT]); (b) washed with 0.1 M cacodylate buffer, pH 7.6; (c) post-fixed in a 3% aqueous solution of osmiumtetroxide (1 h at RT); (d) en bloc stained with 0.5% veronal-buffered uranyl acetate; (e) dehydrated in a graded series of ethanols; (f) infiltrated in a graded series of propylene-oxide/Epon mixtures; and (g) finally embedded in Epon 812 and polymerized for 24 h at 60°C. To facilitate handling and prevent loss, cell suspensions were embedded in 15–20% BSA between aldehyde and osmium fixation as described (3, 16).

Immunolabeling of Ultrathin Sections. Ultrathin Epon sections were mounted on Nickel grids and labeled with the following sequence of immunoreagents (all diluted in PBS with 1% BSA): (a) mouse mAb to DNP (HDP-1, kindly provided by Dr. Fleischman, Washington University, St. Louis, MO) (hybridoma culture supernatant diluted 1:2, 1 h at RT); (b) rabbit anti-mouse IgG (code Z109; Dakopatts, Glostrup, Denmark) (50 μ g/ml, 1 h at RT); and (c) protein A-conjugated to 5- or 10-nm colloidal gold particles (Janssen, Beerse, Belgium) (1:10, 1 h at RT). To minimize background labeling, we found it crucial to centrifuge the gold conjugates before use (5 min, 700 g). After each step, the grids were washed on several drops of PBS/1% BSA for a total of 1 h each time. After the last wash, grids were rinsed in PBS without BSA (10 min at RT) followed by distilled water (5 min at RT). They were then dried and subsequently counterstained with 1% uranyl acetate and 1% lead citrate. Specimens were viewed on an electron microscope (400; Philips Electronic Instruments, Inc., Eindhoven, The Netherlands) at 80 kV.

Results

Neutralization of Acidic Intracellular Compartments Abrogates the Antigen Processing Capacity of Fresh Murine LC. As described previously (6), fLC but not cLC were able to process and present native myoglobin (see Table 1). cLC, though unable to process native myoglobin, were potent in presenting processed forms of the antigen, i.e., defined peptide fragments of myoglobin, to the class II MHC-restricted peptide-specific T cell hybridomas. We now wanted to determine whether acidic compartments were critical for antigen processing by fLC, as is well established for other APC (9–11). The processing capacity of fLC was markedly reduced by chloroquine and monensin, agents known to increase the pH of intracellular compartments (19) and to block antigen processing (11,

Table 1. Chloroquin and Monensin Inhibit Processing of Myoglobin Protein but Do not Block Presentation of Myoglobin Peptide Fragment 110–121

LC	12-h pulse	Antigen during hybridoma assay	Proliferation of CTLL-2 cells					
			10 ⁴	3 × 10 ³	10 ³	3 × 10 ²	10 ²	3 × 10 ¹
			<i>cpm</i> × 10 ⁻³					
Fresh	A Medium only	None	0.2	0.2	0.2	0.2	–	–
	B Medium only	Peptide	104.9	127.4	94.4	30.9	10.3	4.1
	C Medium + myo	None	19.7	20.2	3.7	2.2	0.8	0.4
	D Medium + myo + chlq	None	1.0	0.8	0.5	0.5	0.6	0.8
	E Medium + myo + chlq	Peptide	29.2	50.2	27.5	13.9	3.6	0.8
	F Medium + myo + mon	None	0.2	0.2	0.2	0.2	0.5	0.8
	G Medium + myo + mon	Peptide	11.8	12.6	5.0	3.3	0.9	0.3
Cultured	H Medium only	None	0.2	0.2	0.2	0.1	–	–
	I Medium only	Peptide	55.2	47.7	16.3	2.7	1.5	0.7
	J Medium + myo	None	0.4	0.5	0.4	0.5	0.3	0.2
	K Medium + myo + chlq	None	0.2	0.4	0.4	0.2	0.3	0.5
	L Medium + myo + chlq	Peptide	45.2	64.3	24.7	3.7	1.0	0.2

LC were pulsed with 4 μM myoglobin (*myo*) for 12 h, washed, and tested for presentation of processed protein to the myoglobin peptide-specific hybridoma 11.3.7. IL-2 production by the hybridoma was measured using CTLL-2 indicator cells. Maximal CTLL proliferation with 5 U/ml of human r-IL-2 (Sandoz, Vienna, Austria) was 173.8; background proliferation of CTLL cells was 0.8. Chloroquine (*chlq*) was present at 100 μM; monensin (*mon*) at 25 μM; and the myoglobin peptide 110–121 at 3 μM. Note that cultured LC are not able to process native myoglobin protein into immunogenic peptide fragments (*H* vs. *J*) but are powerful in presenting preprocessed myoglobin peptide fragments to the hybridoma (*I*). The response to peptide is not inhibited by chloroquine pretreatment (*I* vs. *L*). Fresh LC can actively process native myoglobin and present it to the hybridoma (*A* vs. *C*). This response is blocked by chloroquine (*C* vs. *D*) and monensin (*C* vs. *F*). Chloroquine- and monensin-pretreated LC are still able to present peptide to the hybridoma (*E* and *G*).

20). Exposure of fLC or cLC to these agents did not block presentation of the defined myoglobin peptides. These results indicate that acidic organelles are necessary for antigen processing by fLC.

Loss of Antigen Processing Capacity during Culture of Murine LC is Paralleled by Disappearance of Endosomes. Next, we monitored acidic organelles by the DAMP method at the ultrastructural level. Murine fLC exhibited the known cytologic features of LC, including rare LCG (reviewed in reference 21). A variety of membrane-bound compartments concentrated DAMP (see Fig. 1), indicating that they exhibited an acidic pH in the viable state. Included in this category were: (a) electron-lucent vacuoles (average diameter, 0.3 μm) with zero to three intraluminal vesicular profiles exhibiting the appearance of early endosomes (22–26); such structures are termed “multivesicular endosome precursors” and “immature multivesicular endosomes”, respectively, by others (23); (b) electron-lucent vacuoles (average diameter, 0.4 μm) containing multiple intraluminal vesicles corresponding to later stages of endosomes (so-called “multivesicular bodies” or “mature multivesicular endosomes” [22, 23, 25, 26]); (c) lysosomal elements typically with a medium to high density matrix (including occasional phagolysosomes and autophagolysosomes); and (d) the *trans*-Golgi cisternae and associated vesicles, which sometimes appeared labeled, although weakly. Around

the endosomal vacuoles (see above), we sometimes observed tubular, usually DAMP-labeled structures (see Fig. 1 *A*) that may have connected with the large endosomal vacuoles out of the plane of section. Occasionally, comparable tubular structures were encountered in continuity with endosomal vacuoles (see Fig. 1 *A*). Such endosomal vacuolar structures with tubular extensions may correspond to what has been termed compartment of uncoupling of receptor and ligand (CURL) in other cell types (25, 26). LCG (see Fig. 1 *B*), which were typically rare in murine fLC, occasionally showed sparse labeling. It was impossible, however, to unequivocally distinguish this from background labeling.

The density of DAMP labeling, which is roughly proportional to the H⁺ concentration (27), was lowest in the electron lucent vacuoles, intermediate in multivesicular bodies, and highest in lysosomes (see Fig. 1). This is of interest, as in other cell types, endocytosed ligand was found to consecutively enter these increasingly more acidic compartments (19, 28). It was of note that fLC displayed an unusually large number of endosomal elements, in particular of the early type (as identified by morphology and only very sparse gold labeling). Lysosomes were present in variable numbers in fLC.

As described previously, murine cLC differed ultrastructurally from fLC in that they exhibited long surface processes, including the characteristic “veils”, had virtually lost their

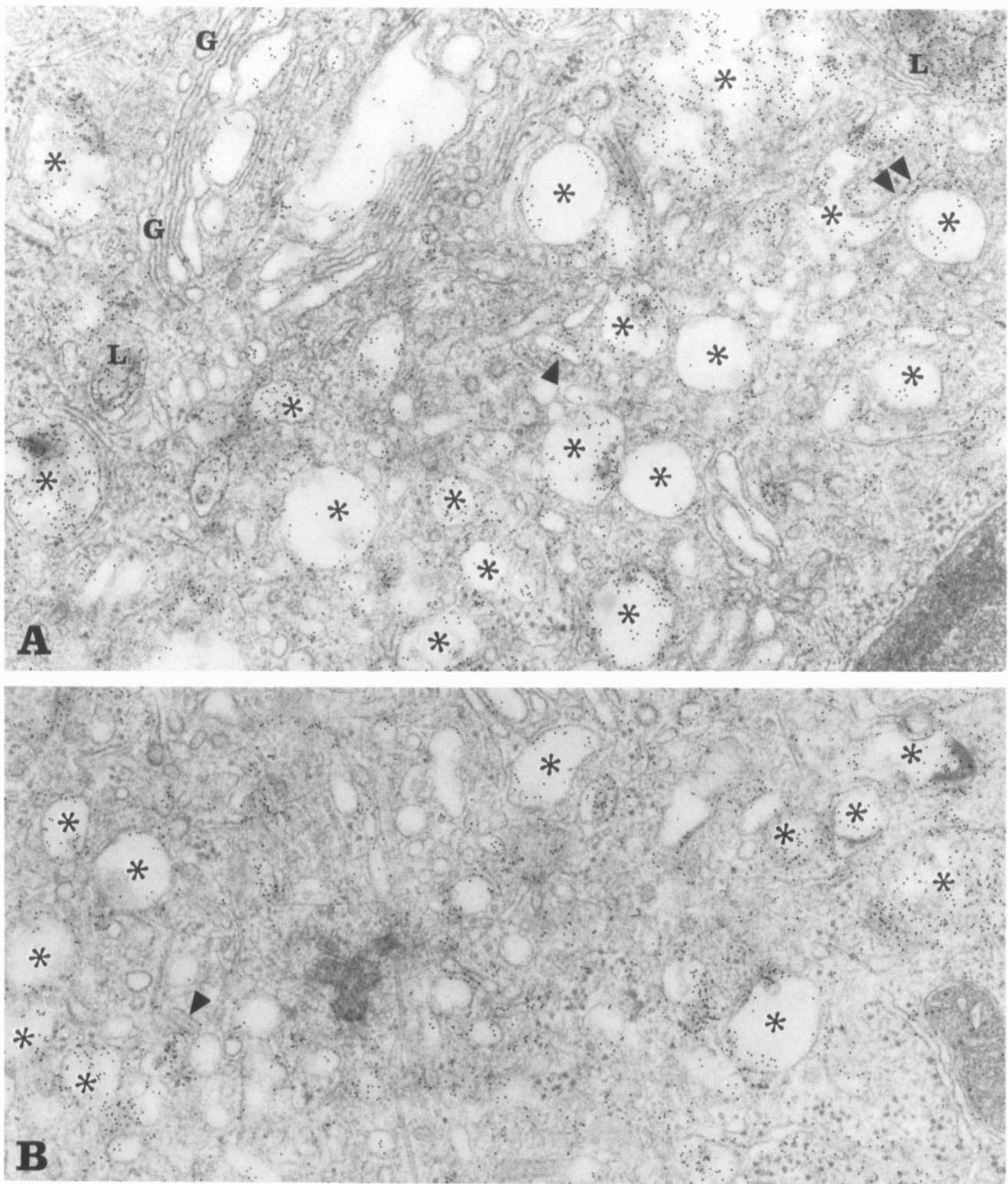


Figure 1. Freshly isolated murine LC: post-embedding detection of acidic compartments (localization of sites of DAMP accumulation by post-embedding immunogold [5-nm] labeling). (A) Asterisks denote DAMP-labeled electron-lucent vacuoles, which represent endosomes and are abundant. Those with intraluminal vesicles and a slightly electron-dense matrix are usually more densely labeled, i.e., more acidic, and likely represent later stages of endosomes. Arrowhead denotes one of the DAMP-labeled, tubular elements, which can be observed in the area around vacuoles. Comparable structures are occasionally seen in continuity with the vacuoles (*double arrowhead*). (L) Lysosomes, which are heavily gold labeled; (G) the *cis* side of a Golgi apparatus. Note that the vesicles and cisternae at the *trans* side are sparsely gold labeled. (B) Asterisks denote DAMP-labeled endosomes. The arrowhead points to a small LCG. (A and B) $\times 50,000$.

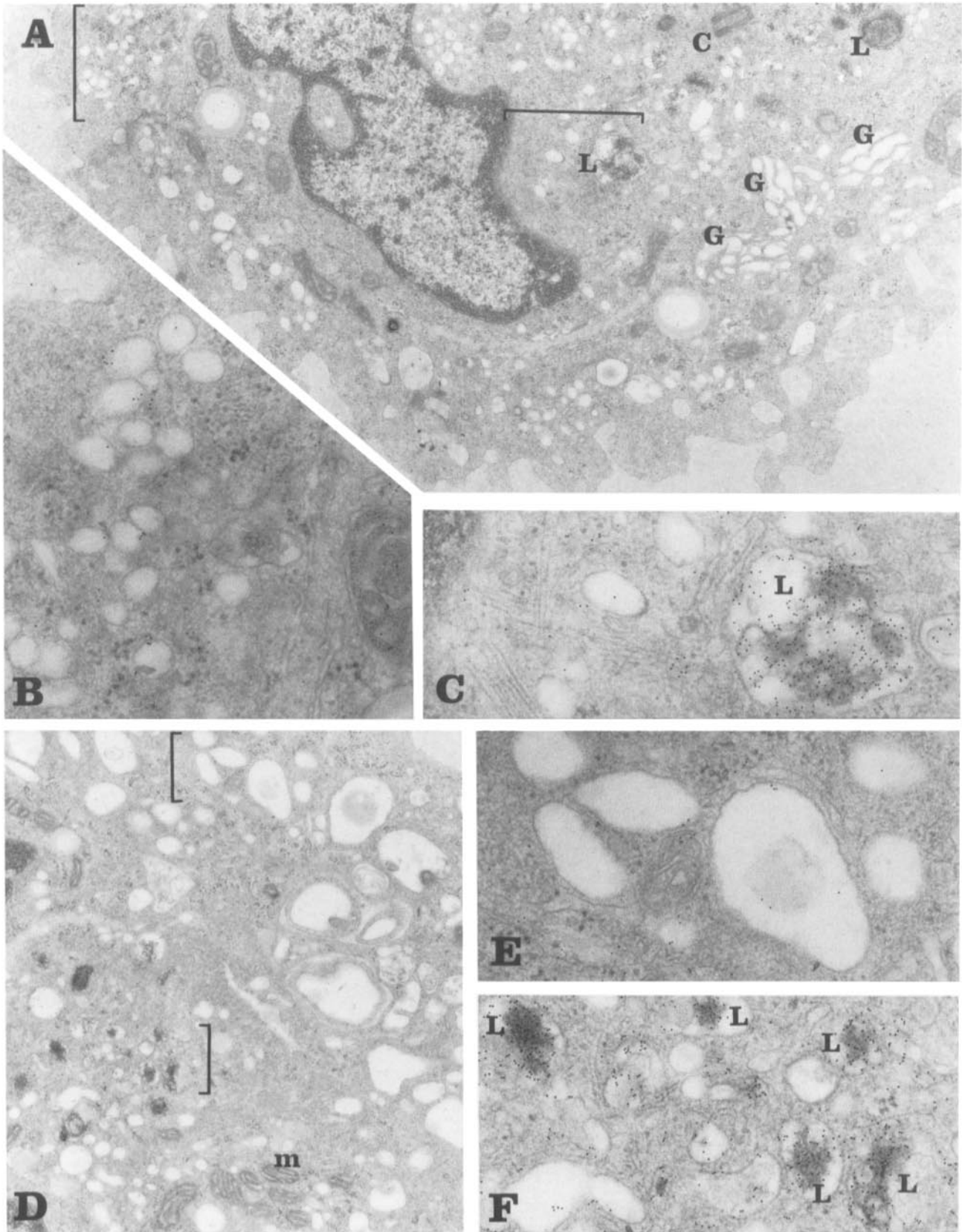


Figure 2. Cultured murine LC: Post-embedding detection of acidic compartments (localization of sites of DAMP accumulation by postembedding immunogold [5-nm] labeling). Two LC are depicted (LC no. 1 = A-C; LC no. 2 = D-F). At low magnification (A), one recognizes Golgi regions (G), a centriole (C), and lysosomal elements (L) in the cytoplasm of LC no. 1. Electron-lucent vesicles/vacuoles are present but most are smaller than those in fresh LC (compare with Fig. 1). High magnifications (respective areas are marked by brackets in A) reveal that these structures are DAMP negative (B), whereas lysosomes (denoted by L in C) display dense 5-nm gold labeling. In LC no. 2 one recognizes at low magnification (D) mitochondria (m), part of the nucleus, and in the cytoplasm electron-lucent vacuoles, and dark-appearing organelles in the center of the cell. At higher magnification (respective areas are marked by brackets in D), one recognizes that most of the electron-lucent vacuoles are not labeled above background (E), whereas the dark-appearing organelles are heavily labeled and represent lysosomes (denoted by L in F). (A and D) $\times 16,000$, (B,C,E, and F) $\times 50,000$.

LCG, and exhibited only an occasional lysosome (3). When we now examined cLC by using the DAMP technique, further differences became apparent (Fig. 2). Most striking was that cLC in contrast to fLC were not rich in endosomes. In particular, early endosomes were rare (Fig. 2). Cultured LC contained also fewer multivesicular bodies, though the difference was less striking. Some cell profiles exhibited a larger number of smaller vesicles, notably at the cell periphery, which were uniformly DAMP negative, and possibly represent pinocytotic vesicles (Fig. 2, A and B). A considerable percentage of cLC exhibited DAMP-labeled structures in the center of the cell corresponding to either prelysosomes (endolysosomes) or lysosomes (see Fig. 2). These usually included "multivesicular bodies" with a rather dense matrix and ghost-like remnants of intraluminal vesicles (such structures have been termed "degenerate multivesicular endosomes" by others [23]), as well as autophagolysosomes (Fig. 2, C and F). Sometimes, small vesicles or tubular profiles, most of them showing a dense core (not shown), also were found to be DAMP positive.

Acidic compartments seem essential for processing by fLC, as shown by blocking with chloroquine or monensin (see above). These maneuvers also abolished DAMP labeling (not shown), indicating that labeling was dependent on acidity (14, 27). Our observation that endosomes disappeared upon culture suggests their involvement in antigen processing.

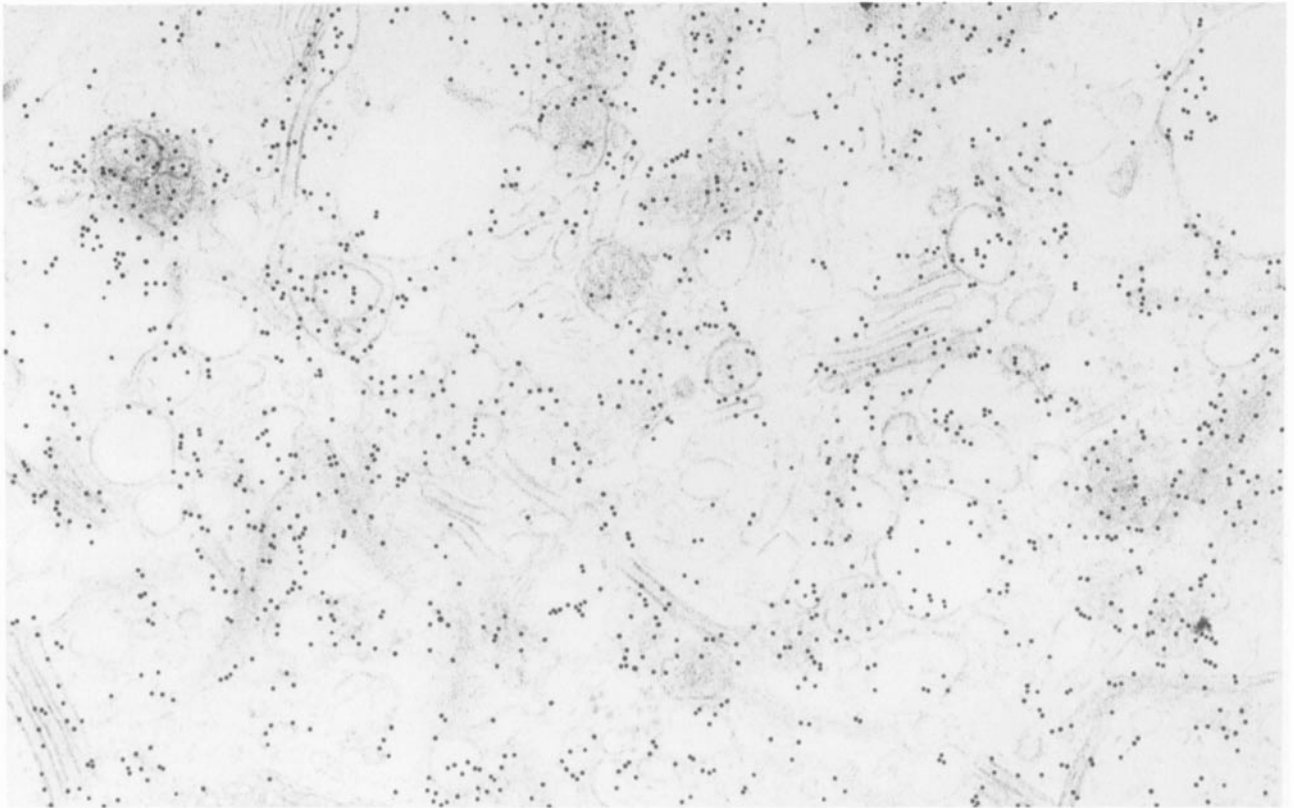
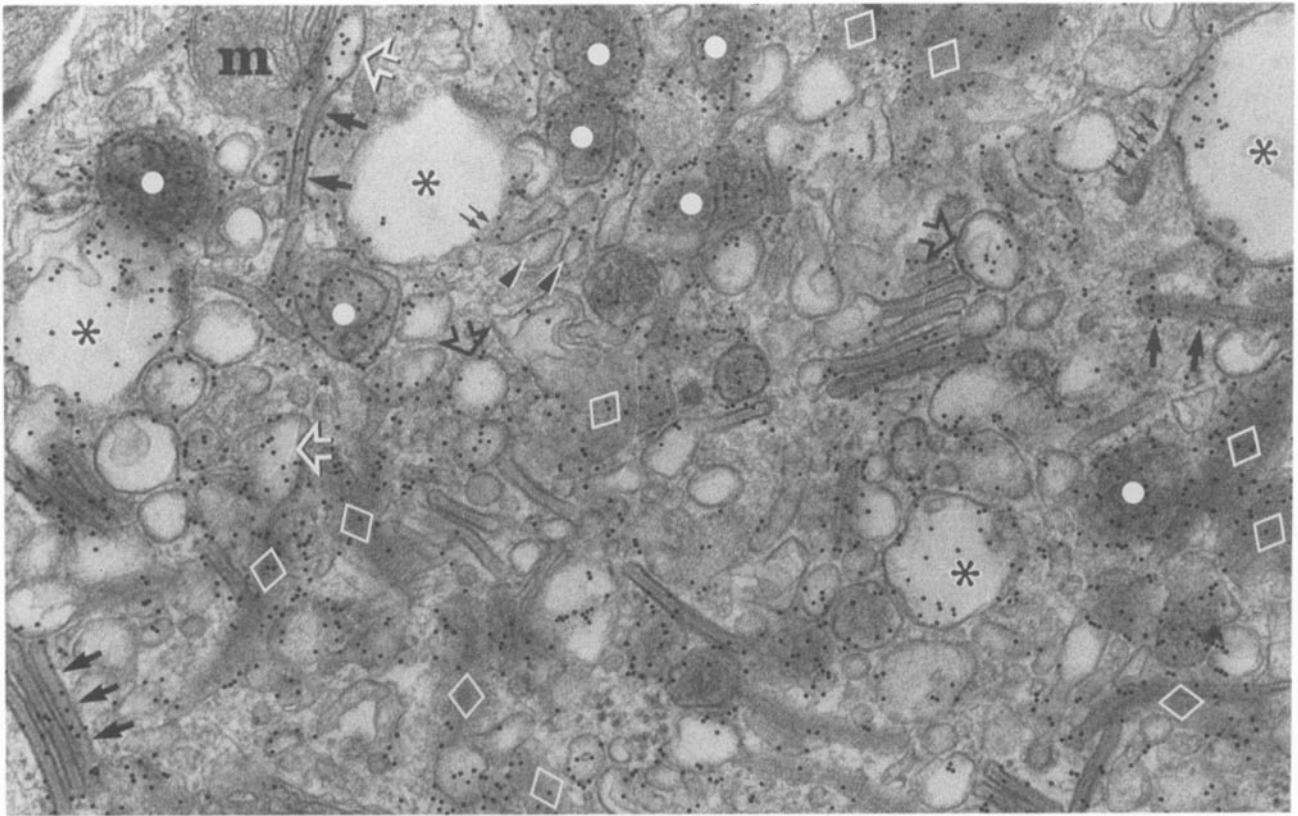
The Study of Human LC Reveals that LCG in Part Exhibit an Acidic pH in Fresh LC, and that Acidic LCG as Well as Endosomes Disappear During Culture. Available evidence indicates that human LC change during culture like murine ones, and come to resemble lymphoid DC in phenotype and T cell stimulatory capacity (16, 29). Whether human LC lose their antigen processing capacity like murine LC upon culture is, however, not yet known. We were nevertheless interested to study human fresh and cultured LC by the DAMP technique, as we hoped to learn more about LCG ("Birbeck Granules"). Human LC possess many more and better developed LCG than murine ones (21, 30). Upon culture, LCG become smaller and are reduced in number, but not completely disappear as in murine LC (16, 29).

When studying human fLC (in viable epidermal sheets) by the DAMP technique, we were surprised by the abundance of acidic compartments (Figs. 3 and 4). Sparsely DAMP-labeled electron-lucent vacuoles (diameter, 0.3–0.8 μm , with or without intraluminal vesicles, i.e., endosomes) were always present, but usually were not as numerous as in murine fLC (Figs. 3 and 4, B and C). As in murine LC, we observed tubular elements around endosomal vacuoles, which sometimes were found in continuity with the vacuoles (Figs. 3

and 4 C). These structures may therefore correspond to vacuolar and tubular elements of CURL described in other cell types (25, 26). Rod portions of LCG, even when tangentially or obliquely sectioned, could easily be identified, and were abundant in most LC profiles (Figs. 3 and 4). A variable portion (from 10 to 50% on a given section) of the LCG rods appeared gold labeled, and the remainder was clearly unlabeled (Figs. 3 and 4 A). Part of the LCG rods opened into vesicles, giving the LCG the classical tennis racket-like appearance (Fig. 3). Usually, the rod as well as the vesicular portion, appeared DAMP labeled, but the labeling of the rod usually appeared more dense (Figs. 3 and 4). This might indicate a higher amount of accumulated DAMP molecules and a more acidic pH, or just reflect a higher number of available crosslinking sites in the dense rod portions (27). In between the rod portions electron-lucent noncoated vesicles were frequently labeled (Fig. 3), and likely corresponded to cross-sectioned vesicular portions of LCG. Some of the rods of LCG opened into vesicles larger than the usual vesicular portions of LCG (Figs. 4, B and C). These vacuoles in part contained intraluminal vesicular profiles, were all sparsely DAMP labeled, and corresponded to the endosomes described above. Among hundreds of cell profiles examined, only two LCG were found attached to the cell membrane (one of them exhibiting a fuzzy coat at the distal end), and appeared unlabeled (not shown). For a detailed discussion on the relevance of membrane-attached vs. intracellular LCG, see reference 21. Fresh human LC displayed a surprisingly large number of lysosomes (see Figs. 3 and 4 A). As in murine fLC, we occasionally found *trans*-Golgi cisternae, as well as associated vesicles DAMP labeled. This is of interest as so far, the *trans*-cisternae have been described as being acidic only in fibroblasts and hepatocytes, though all cells examined so far have acidic *trans*-Golgi vesicles (27).

Cultured human LC displayed the ultrastructure we have described previously (16). By DAMP labeling, as in the mouse, a difference in the number as well as quality of acidic compartments was readily apparent when compared with fLC (Fig. 5). Electron-lucent vacuoles were occasionally encountered, but usually were DAMP negative, and thus did not qualify as endosomes (Fig. 5 C). As compared with fLC, LCG were markedly reduced in number and were generally much less prominent, appearing as short rods (Fig. 5 C). Only very occasionally did such a rod appear sparsely DAMP labeled. A substantial portion of cLC profiles exhibited densely labeled phagolysosomes and autophagolysosomes (Fig. 5). Interestingly, however, typical lysosomes with a dense homogeneous matrix, though rather plentiful in fLC (see Figs. 3 and

Figure 3. Intraepidermal human LC: post-embedding detection of acidic compartments (localization of sites of DAMP accumulation by post-embedding immunogold [10-nm] labeling). Upper and lower panels are prints made from the same negative, but for the lower panel, a short exposure time was used to reveal mainly the 10-nm gold particles. Note that the gold particles show a nonrandom distribution and the following structures are labeled above background: (a) most of the LCG, including rod portions (some of them denoted by *black arrows*), many of which are tangentially sectioned (*white rhombus*); some of the LCG rods open into vesicles (*open white arrows*), giving the LCG the classical tennis racket-like appearance; in between the rod portions, vesicles were frequently labeled (*open black arrows*), and likely corresponded to cross-sectioned vesicular portions of LCG; (b) sparsely labeled electron-lucent vacuoles (with or without intraluminal vesicles), i.e., endosomes, which are marked by asterisks; (c) tubular elements in the vicinity of endosomal vacuoles (*arrowheads*), which are sometimes in continuity with endosomes (*small black arrows*); (d) densely labeled lysosomes (*white dots*). (m) Mitochondria. ($\times 50,000$).



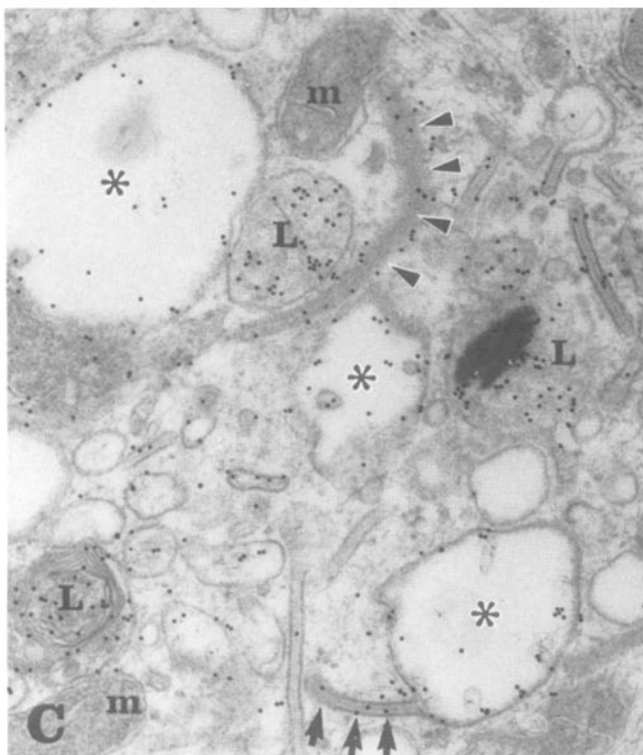
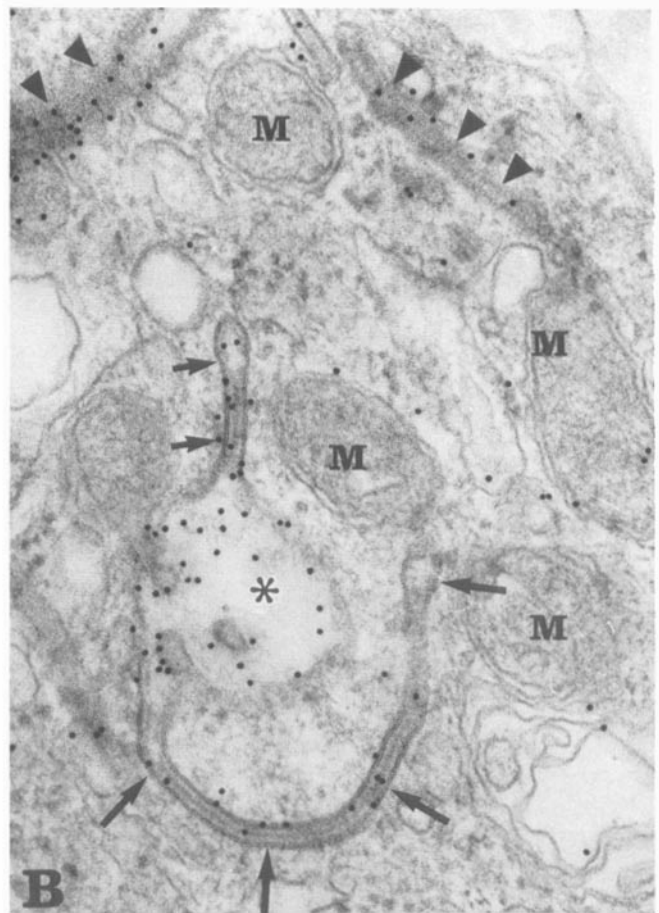
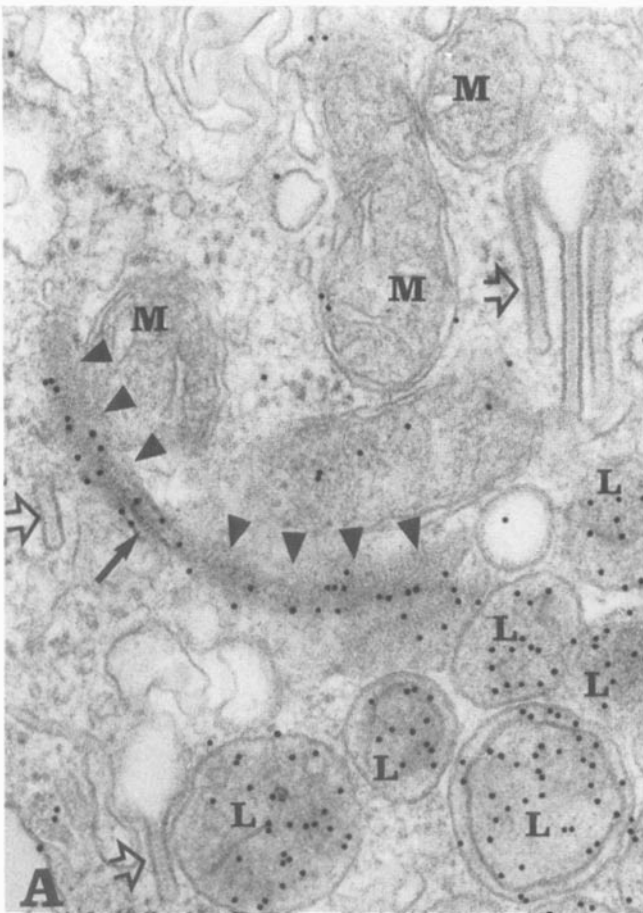


Figure 4. Intraepidermal human LC: post-embedding detection of acidic compartments (localization of sites of DAMP accumulation by post-embedding immunogold [10-nm] labeling). (A) In this part of the cytoplasm of a LC, one sees a DAMP-positive LCG rod, which over most of its length is tangentially sectioned (*arrowheads*) (note characteristic cross-striation), but at one point is cross-sectioned (*arrow*). The vesicle to the right of the LCG rod likely represents the vesicular portion of the LCG which connects to the rod out of the plane of section. Open arrows mark DAMP-negative LCG, (L) DAMP-positive lysosomes; (M) mitochondria. ($\times 65,000$). (B) Here one sees tangentially or obliquely sectioned, DAMP-labeled LCG rods (*arrowheads*), as well as two cross-sectioned LCG rods (*short and long arrows*) communicating with an endosome (*asterisk*). ($\times 65,000$). (C) Note DAMP-labeled endosomes (*asterisks*), one of which is in continuity with a LCG rod (*black arrows*). *Arrowheads* denote tangentially sectioned, gold-labeled rod portion of a LCG. Three DAMP-positive lysosomes (L) are seen, as well as several small vesicles and a tubular profile, which are gold labeled and may correspond to cross-sectioned vesicular profiles or tubular extensions of endosomes similar to those in Fig. 3. Mitochondria (m) are not labeled. ($\times 50,000$)

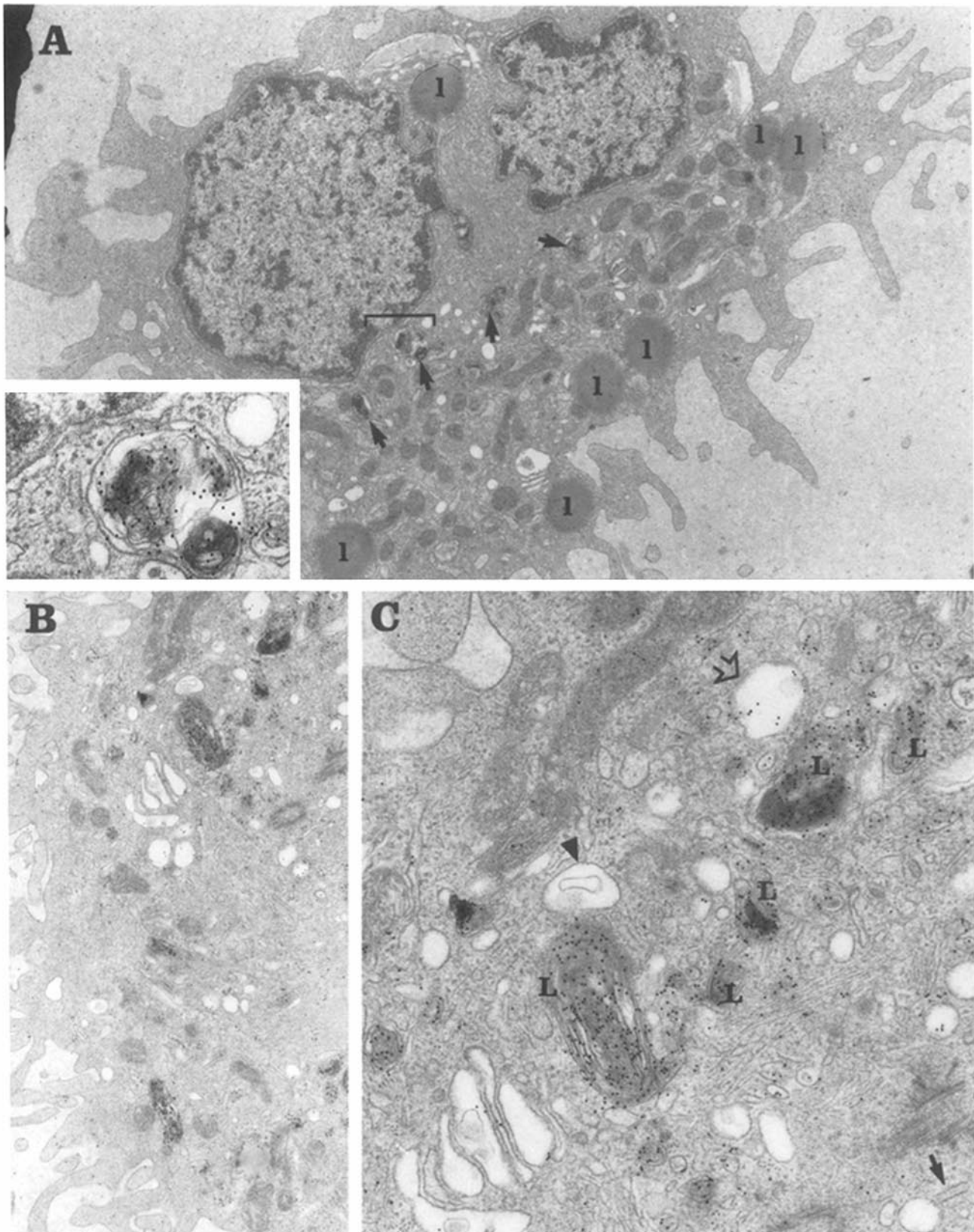


Figure 5. Cultured human LC post-embedding detection of acidic compartments (localization of sites of DAMP accumulation by post-embedding immunogold [10-nm] labeling). Two cultured LC are shown (LC no. 1 [A]; LC no. 2 [B and C]). At low magnification of LC no. 1 (A), one notes the characteristic thin cytoplasmic sheets (so-called “veils”) extending from the cell surface, many mitochondria, lipid droplets (l), as well as dark-appearing organelles (arrows), which appear gold labeled. Inset shows the area marked by a bracket at higher magnification, and confirms that the dark organelles are DAMP positive, and represent lysosomal elements. Note that electron-lucent vacuoles are not present in contrast to fLC (see Figs. 3 and 4). LCG were not encountered in this LC profile. $\times 12,000$; $\times 50,000$ (inset). In LC no. 2, only few electron-lucent vesicles/vacuoles are seen (B). Candidate endosomal structures at higher magnification (C) are occasionally sparsely labeled (open arrow), but usually are not labeled above background (arrowhead). In this LC profile, a few LCGs were encountered, which were, however, much shorter than those in fLC (see Figs. 3 and 4) and appeared unlabeled (black arrow). Lysosomal elements (L) were clearly labeled. (A) $\times 16,000$; (B) $\times 40,000$.

4 A), were almost never encountered. Like in the mouse, we occasionally observed densely labeled small vesicles or tubular profiles with dense cores in the center of human cLC. In control specimens (27) treated with monensin or chloroquine, DAMP labeling was abolished, indicating that DAMP labeling was due to acidity.

Discussion

The study of epidermal LC has helped to understand the relationship between DC found in peripheral tissues and those in lymphoid organs. In addition, LC prove a rewarding model to address basic questions of accessory cell function. This is due to the fact that antigen processing and sensitizing functions are reciprocally expressed in fresh vs. cultured LC (6, 7). Studying LC helped to identify antigen-independent clustering as a critical feature of DC. This unique capacity is acquired by LC during their maturation into potent immunostimulatory DC in culture (reviewed in references 2 and 4), and now awaits elucidation of its molecular mechanism. In the current study, we have shown that LC might also prove useful to study certain aspects of antigen processing. Our observation that in murine LC the downregulation of antigen processing capacity is paralleled by a disappearance of endosomes, notably those of the early type, suggests that these organelles are critical for antigen processing by fLC. Although endosomes from studies in other cell types are generally believed to be critical in antigen processing (12, 13), it is not yet settled in which subpopulations of endosomes (28) processing events take place. Studies using cells with defective acidification have suggested early endosomes as candidates (13). This is also supported by the observation in other model systems that endocytosed transferrin, which recycles through early endosomes (28), interacts with freshly synthesized class II molecules (31, 32). It has also been demonstrated that both transferrin and class II molecules can be internalized into early endosomes (33). LC may be an optimal model system to determine where exactly antigen and class II molecules interact. In this context, it is noteworthy that the synthesis of class II molecules is high in fLC, but switched off in cultured LC (Kämpgen et al., manuscript in preparation).

The study of murine LC was inconclusive with regard to DAMP labeling of LCG (Birbeck Granules), which are scarce even in fresh murine LC. Though we do not yet know whether human LC downregulate antigen processing like murine ones, we chose to study human LC, as they possess more and larger LCG than murine ones. Our finding that 10–50% of LCG in fresh human LC were acidic is an interesting new feature of this morphologically highly characteristic, but enigmatic marker organelle of epidermal LC (21, 30). It further supports the idea that LCG might be involved in antigen processing. Such a thought arose from the observation that upon culture, murine LC lose the capability to process native myoglobin (6) as well as LCG (3). In congruence with the proposal of LCG as antigen-processing organelles are also recent immunolabeling experiments suggesting that membrane-bound molecules after endocytosis can reach intracellular LCG (34–36, and reviewed in 21). Our observation that only a variable portion of LCG was DAMP positive cannot be definitely explained at present. We found LCG in continuity with endosomes, and the respective LCG were always DAMP labeled. It is, therefore, tempting to speculate that all the DAMP-positive LCG communicate with endosomes, albeit usually at a level not included within a given ultrathin section. DAMP-negative LCG might be nonacidic because they have already pinched off from, or alternatively, not yet fused with endosomes. This interpretation would assume that only the endosomal membranes but not the LCG possess a proton pump (19, 27). The origin and fate of LCG is not yet settled (for a detailed discussion of this disputed issue see reference 21). We currently favor the hypothesis that LCG derive from endosomes, possibly representing a tubular portion of CURL with a unique morphology (i.e., a central linear density).

Antigen processing is a multistep procedure and could be altered at various stages, such as uptake, proteolysis, and/or binding to MHC molecules. Recent studies using the fluorescent tracer rhodamin-OVA indicate that both fLC and cLC pinocytose protein into intracellular granules (37). After uptake, an acidic compartment is important for processing. We postulate that the failure of cLC to process antigen is not due to a lack of uptake, but instead reflects an absence of certain acidic organelles (endosomes and LC granules).

We thank the colleagues who provided us with valuable reagents (see Materials and Methods). We appreciate the help of Drs. H. Anderl and C. Papp at the Department of Plastic Surgery, University of Innsbruck, who provided us with human skin specimens, as well as the photographic skills of B. Sickert. For continued support, we thank Dr. P. Fritsch, Department of Dermatology, University of Innsbruck.

This work was supported by the Austrian Science Foundation (FWF grants P6170M and P7285M to G. Schuler). E. Kämpgen was supported by a postdoctoral fellowship from the Deutsche Forschungsgemeinschaft (Ka753/1-1).

Address correspondence to Gerold Schuler, Department of Dermatology, University of Innsbruck, Anichstrasse 35, A-6020 Innsbruck, Austria.

Received for publication 25 June 1990.

References

1. MacPherson, G.G. 1989. Lymphoid dendritic cells: their life history and roles in immune responses: 28th Forum in Immunology. *Res. Immunol.* 140:877.
2. Steinman, R.M., and K. Inaba. 1989. Immunogenicity and role of dendritic cells. *Bioessays.* 10:145.
3. Schuler, G., and R.M. Steinman. 1985. Murine epidermal Langerhans cells mature into potent immunostimulatory dendritic cells in vitro. *J. Exp. Med.* 161:526.
4. Romani, N., M. Witmer-Pack, M. Crowley, S. Koide, G. Schuler, K. Inaba, and R.M. Steinman. 1990. Langerhans cells as immature dendritic cells. In *Epidermal Langerhans Cells*. G. Schuler, editor. CRC Press, Inc., Boca Raton, FL. In press.
5. Romani, N., and G. Schuler. 1989. Structural and functional relationships between epidermal Langerhans cells and dendritic cells. *Res. Immunol.* 140:895.
6. Romani, N., S. Koide, M. Crowley, M. Witmer-Pack, A.M. Livingstone, C.G. Fathman, K. Inaba, and R.M. Steinman. 1989. Presentation of exogenous protein antigens by dendritic cells to T cell clones: intact protein is presented best by immature epidermal Langerhans cells. *J. Exp. Med.* 169:1169.
7. Streilein, J.W., and S.F. Grammer. 1989. In vitro evidence that Langerhans cells can adopt two functionally distinct forms capable of antigen presentation to T lymphocytes. *J. Immunol.* 143:3925.
8. Aiba, S., and S.I. Katz. 1990. Cultured Langerhans cells can process and present intact protein antigens. *J. Invest. Dermatol.* 94:503 (Abstr.).
9. Pernis, B., S.C. Silverstein, and H.J. Vogel. 1988. Processing and Presentation of Antigens. Academic Press, San Diego. 324 pp.
10. Germain, R.N. 1986. The ins and outs of antigen processing and presentation. *Nature (Lond.)* 322:687.
11. Unanue, E.R. 1984. Antigen-presenting function of the macrophage. *Annu. Rev. Immunol.* 2:395.
12. Blum, J.S., R. Diaz, S. Diment, M. Fiani, L. Mayorga, J.S. Rodman, and P.D. Stahl. 1989. Proteolytic processing in endosomal vesicles. In *Immunological Recognition*. Cold Spring Harbor Laboratory Press, Cold Spring Harbor, New York. 287 pp.
13. McCoy, K.L., J. Miller, M. Jenkins, F. Ronchese, R.N. Germain, and R.H. Schwartz. 1989. Diminished antigen processing by endosomal acidification mutant antigen-presenting cells. *J. Immunol.* 143:29.
14. Anderson, R.G.W., J.R. Falck, J.L. Goldstein, and M.S. Brown. 1984. Visualization of acidic organelles in intact cells by electron microscopy. *Proc. Natl. Acad. Sci. USA.* 81:4838.
15. Koch, F., C. Heufler, E. Kämpgen, D. Schneeweiss, G. Böck, and G. Schuler. 1990. Tumor necrosis factor α maintains the viability of murine epidermal Langerhans cells in culture but in contrast to granulocyte/macrophage colony-stimulating factor without inducing their functional maturation. *J. Exp. Med.* 171:159.
16. Romani, N., A. Lenz, H. Glassl, H. Stössel, U. Stanzl, O. Majdic, P. Fritsch, and G. Schuler. 1989. Cultured human Langerhans cells resemble lymphoid dendritic cells in phenotype and function. *J. Invest. Dermatol.* 93:600.
17. Foster, C.A., H. Yokozeki, K. Rappersberger, F. Koning, B. Volc-Platzter, A. Rieger, J.E. Coligan, K. Wolff, and G. Stingl. 1990. Human epidermal T cells predominantly belong to the lineage expressing α/β T cell receptor. *J. Exp. Med.* 171:997.
18. Morel, P.A., A.M. Livingstone, and C.G. Fathman. 1987. Correlation of the T cell receptor V β gene family with MHC restriction. *J. Exp. Med.* 166:583.
19. Mellman, I., R. Fuchs, and A. Helenius. 1986. Acidification of the endocytic and exocytic pathways. *Annu. Rev. Biochem.* 55:663.
20. Chesnut, R.W., S.M. Colon, and H.M. Grey. 1982. Requirements for the processing of antigens by antigen-presenting B cells. I. Functional comparison of B cell tumors and macrophages. *J. Immunol.* 129:2382.
21. Schuler, G., N. Romani, H. Stössel, and K. Wolff. 1990. Structural organization and biological properties of Langerhans cells. In *Epidermal Langerhans cells*. G. Schuler, editor. CRC Press, Inc., Boca Raton, FL. In press.
22. Willingham, M.C., and I. Pastan. 1984. Endocytosis and exocytosis: current concepts of vesicle traffic in animal cells. *Int. Rev. Cytol.* 92:51.
23. Harding, C., M.A. Levy, and P. Stahl. 1985. Morphological analysis of ligand uptake and processing: the role of multivesicular endosomes and CURL in receptor-ligand processing. *Eur. J. Cell Biol.* 36:230.
24. Hopkins, C.R., and I.S. Trowbridge. 1983. Internalization and processing of transferrin and the transferrin receptor in human carcinoma A431 cells. *J. Cell Biol.* 97:8508.
25. Geuze, H.J., J.W. Slot, and A.L. Schwartz. 1987. Membranes of sorting organelles display lateral heterogeneity in receptor distribution. *J. Cell Biol.* 104:1715.
26. Geuze, H.J., J.W. Slot, G.J.A.M. Strous, H.F. Lodish, and A.L. Schwartz. 1983. Intracellular site of asialoglycoprotein receptor-ligand uncoupling: double-label immunoelectron microscopy during receptor-mediated endocytosis. *Cell.* 32:277.
27. Anderson, R.G.W., and L. Orci. 1988. A view of acidic intracellular compartments. *J. Cell Biol.* 106:539.
28. Schmid, S.L., R. Fuchs, P. Male, and I. Mellman. 1988. Two distinct subpopulations of endosomes involved in membrane recycling and transport to lysosomes. *Cell.* 52:73.
29. Teunissen, M.B.M., J. Wormeester, S.R. Krieg, P.J. Peters, I.M.C. Vogels, M.L. Kapsenberg, and J.D. Bos. 1990. Human epidermal Langerhans cells undergo profound morphological and phenotypic changes during in vitro culture. *J. Invest. Dermatol.* 94:166.
30. Wolff, K. 1972. The Langerhans cell. *Curr. Probl. Dermatol.* 4:79.
31. Cresswell, P. 1985. Intracellular class II HLA antigens are accessible to transferrin-neuraminidase conjugates internalized by receptor-mediated endocytosis. *Proc. Natl. Acad. Sci. USA.* 82:8188.
32. Cresswell, P., and J.S. Blum. 1988. Intracellular transport of class II HLA antigens. In *Processing and Presentation of Antigens*. B. Pernis, S.C. Silverstein, and H.J. Vogel, editors. Academic Press, Inc., San Diego. 43-51.
33. Harding, C.V., and E.R. Unanue. 1989. Antigen processing and intracellular Ia: possible roles of endocytosis and protein synthesis in Ia function. *J. Immunol.* 142:12.
34. Hanau, D., M. Fabre, D.A. Schmitt, J.-C. Garaud, G. Pauly, M.-M. Tongio, S. Mayer, and J.-P. Cazenave. 1987. Human epidermal Langerhans cells coinitalize by receptor-mediated endocytosis "nonclassical" major histocompatibility complex class I molecules (T6 antigens) and class II molecules (HLA-DR antigens). *Proc. Natl. Acad. Sci. USA.* 84:2901.
35. Hanau, D., M. Fabre, D.A. Schmitt, J.-L. Stampf, J.-C. Garaud, T. Bieber, E. Grosshans, C. Benezra, and J.-P. Cazenave. 1987. Human epidermal Langerhans cells internalize by receptor-

- mediated endocytosis T6 (CD1 "NA1/34") surface antigen. Birbeck granules are involved in the intracellular traffic of the antigen. *J. Invest. Dermatol.* 89:172.
36. Takigawa, M., K. Iwatsuki, M. Yamada, H. Okamoto, and S. Imamura. 1985. The Langerhans cell granule is an adsorptive endocytic organelle. *J. Invest. Dermatol.* 85:12.
37. Puré, E., K. Inaba, M.T. Crowley, L. Tardelli, M.D. Witmer-Pack, G. Ruberti, C. G. Fathman, and R. M. Steinman. 1990. Antigen processing by epidermal Langerhans cells correlates with the level of biosynthesis of MHC class II molecules and expression of invariant chain. *J. Exp. Med.* 172:1459.